Journal of Colloid and Interface Science 672 (2024) 244–255

Contents lists available at ScienceDirect

Journal of Colloid And Interface Science

journal homepage: www.elsevier.com/locate/jcis

Modulating protein unfolding and refolding via the synergistic association of an anionic and a nonionic surfactant

Johanna Hjalte [a], Carl Diehl [b], Anna E. Leung [c], Jia-Fei Poon [a,c], Lionel Porcar [d], Rob Dalgliesh [e], Helen Sjögren [f], Marie Wahlgren [a], Adrian Sanchez-Fernandez [g,*]

[a] Food Technology, Engineering and Nutrition, Lund University, Box 124, 221 00 Lund, Sweden
[b] SARomics Biostructures AB, Medicon Village, Scheelevägen 2, 223 81 Lund, Sweden
[c] European Spallation Source, Box 176, 221 00 Lund, Sweden
[d] Institut Laue-Langevin, 71 Avenue des Martyrs, 38000 Grenoble, France
[e] ISIS Neutron and Muon Source, Science and Technology Facilities Council, Rutherford Appleton Laboratory, Didcot OX11 0QX, UK
[f] Ferring Pharmaceuticals A/S, Amager Strandvej 405, 2770 Kastrup, Denmark
[g] Center for Research in Biological Chemistry and Molecular Materials (CIQUS), Department of Chemical Engineering, Universidade de Santiago de Compostela, Santiago de Compostela 15705, Spain

GRAPHICAL ABSTRACT

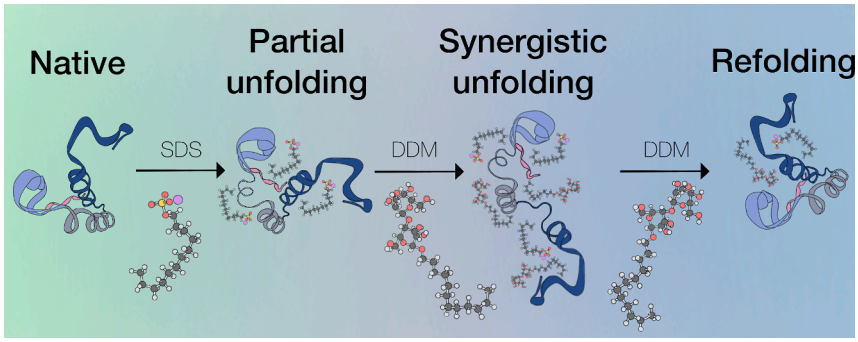

ABSTRACT

Hypothesis: Nonionic surfactants can counter the deleterious effect that anionic surfactants have on proteins, where the folded states are retrieved from a previously unfolded state. However, further studies are required to refine our understanding of the underlying mechanism of the refolding process. While interactions between nonionic surfactants and tightly folded proteins are not anticipated, we hypothesized that intermediate stages of surfactant-induced unfolding could define new interaction mechanisms by which nonionic surfactants can further alter protein conformation.

Experiments: In this work, the behavior of three model proteins (human growth hormone, bovine serum albumin, and β-lactoglobulin) was investigated in the presence of the anionic surfactant sodium dodecylsulfate, the nonionic surfactant β-dodecylmaltoside, and mixtures of both surfactants. The transitions occurring to the proteins were determined using intrinsic fluorescence spectroscopy and far-UV circular dichroism. Based on these results, we developed a detailed interaction model for human growth hormone. Using nuclear magnetic resonance and contrast-variation small-angle neutron scattering, we studied the amino acid environment and the conformational state of the protein.

Findings: The results demonstrate the key role of surfactant cooperation in defining the conformational state of the proteins, which can shift away or toward the folded state depending on the nonionic-to-ionic surfactant ratio. Dodecylmaltoside, initially a non-interacting surfactant, can unexpectedly associate with sodium

* Corresponding author.
E-mail address: adriansanchez.fernandez@usc.es (A. Sanchez-Fernandez).

https://doi.org/10.1016/j.jcis.2024.05.157
Received 2 April 2024; Received in revised form 3 May 2024; Accepted 21 May 2024
Available online 22 May 2024

dodecylsulfate-unfolded proteins to further impact their conformation at low nonionic-to-ionic surfactant ratio. When this ratio increases, the protein begins to retrieve the folded state. However, the native conformation cannot be fully recovered due to remnant surfactant molecules still adsorbed to the protein. This study demonstrates that the conformational landscape of the protein depends on a delicate interplay between the surfactants, ultimately controlled by the ratio between them, resulting in unpredictable changes in the protein conformation.

1. Introduction

By mimicking Nature's ability to control certain protein functions through specific interactions with amphipathic molecules [1], protein behavior can be modulated in artificial systems by altering the interaction landscape through the addition of surfactants [2]. Interactions between proteins and surfactants are important in a wide range of applications and a variety of products. In cleaning detergents, enzymes and surfactants co-exist to improve detergency [3]. In pharmaceutical formulation, nonionic surfactants protect proteins from surface-induced aggregation by hindering their access to interfaces without altering the compact fold of the proteins [4]. As a rule of thumb, anionic surfactants bind to and unfold proteins, which is exploited in analytical and separation methods such as SDS-PAGE [5]. Therefore, the broad protein-surfactant interaction landscape contributes to either enhancing or disrupting the conformational and colloidal stability of the protein, as well as to affecting its function [6]. However, despite continuous efforts over the years, a general mechanistic model for protein-surfactant interactions, particularly those involving surfactant mixtures, remains elusive.

Due to their importance in fundamental and applied sciences, surfactant–protein interactions have been studied for decades. Early studies showed that the surfactant-to-protein molar ratio drives conformational changes rather than absolute surfactant concentrations [7,8]. In addition, the extent of saturation of the hydrophobic patches on the protein surface controls the protective effect of nonionic surfactants against aggregation, rather than the surfactant CMC [9]. Trends related to extrinsic factors have also been identified; protein-surfactant systems comprise a collection of equilibria that are sensitive to, e.g., temperature, pH, and ionic strength [10,11]. Besides, the expected interaction depends on both the protein and surfactant in question. For instance, the loosely folded α–lactalbumin can be unfolded by maltoside-based nonionic surfactants [12], whereas uncharged amphiphiles marginally bind to compactly folded proteins [2]. Surfactant binding can either induce changes that are thermodynamically stable and easy to detect or in the form of transient exchanges that are more challenging to determine experimentally [2,13]. In recent years, experimental (e.g., spectroscopy, scattering, and calorimetry) and computational studies have led the way toward to a set of principles for understanding the realm of surfactant–protein interactions [6,14–16].

A recurrent aspect in many investigations is that interactions between surfactants and proteins are dynamic and reversible, which can be utilized to achieve refolding of previously surfactant-unfolded proteins [13,17–24]. For instance, the addition of an ionic surfactant (often sodium dodecyl sulfate, SDS) unfolds the protein. Subsequently, a nonionic surfactant (e.g., β-dodecylmaltoside, DDM) is added at a concentration above its CMC to refold the protein. The general picture suggests that the presence of nonionic micelles displaces the ionic surfactant to the micellar phase, causing the protein to retrieve (either partially or totally) its native conformation [18,25]. Therefore, the chemical variety of surfactants enables a synthetically accessible approach to develop refolding methods tailored for specific systems, finding potential applications in recombination biotechnology [19], new formulation methods [20], and biomaterials with programmable properties [21]. However, the mechanism of the dynamic interaction between protein and surfactant pairs is still not fully understood, and mapping this constitutes an important step toward predesigning these systems and increasing their applicability.

To elucidate the structural phases and interactions of the system, three model proteins were systematically studied: human growth hormone (hGH), bovine serum albumin (BSA), and β-lactoglobulin (βLG). These three proteins constitute valuable models due to several reasons: (1) the proteins present a negative charge at pH = 7.0, which avoids threatening colloidal stability upon addition of the anionic SDS [24,26], (2) they are known to populate a broad conformational landscape upon SDS addition [26–28], (3) the proteins have different sizes and secondary structures, which allow to determine whether these parameters contribute to protein-surfactant interactions (Fig. 1a). SDS was used as the ionic surfactant to induce protein denaturation [10,27,29–31], where the protein-to-surfactant ratio can be used to isolate different structural phases. The nonionic surfactant DDM was used as the partner for protein refolding [13]. The interaction stages were investigated by titration fluorescence spectroscopy upon the addition of the surfactants at different molar ratios (i.e., DDM:SDS:protein, with a nominal value of 1 for the protein). In addition, the transitions occurring in the secondary structure of the proteins were studied using far-UV circular dichroism (CD). Once key transitions were identified, the local environment of the hGH backbone was studied by proton nuclear magnetic resonance spectroscopy (^{1}H NMR), and detailed structural models of the hGH conformation were built using contrast-variation small-angle neutron scattering (SANS). Our results reveal that the unfolding/refolding process in the presence of surfactant pairs cannot be simply understood in terms of isolated interactions with each individual amphiphile. Instead, the synergistic association of the two surfactants with the protein determines the mechanism of unfolding and refolding. As such, the contributions from the nonionic surfactant can drive the process either away or toward the native fold depending on the initial conformational state of the protein and the proportion of charged and uncharged surfactants in the system. Notably, this investigation reveals that the native fold of the protein is not fully retrieved even at exceedingly high DDM/SDS ratios, suggesting that a few surfactant molecules remain entrapped in the protein envelope upon refolding.

2. Materials and methods

2.1. Materials

Sodium phosphate monobasic and dibasic (Reag. Ph Eur, Sigma-Aldrich, US), sodium hydroxide (>99.99 %, Sigma-Aldrich), sodium azide (Reag. Ph Eur, Scharlab, Spain), SDS (ACS reagent, Sigma-Aldrich, US), DDM (≥99 %, Anatrace, US), and D_2O (99.9 %D, Sigma-Aldrich) were used as received. Highly pure hGH was kindly supplied by Ferring Pharmaceuticals A/S (Kastrup, Denmark) as a lyophilized powder. BSA (>98 %) and βLG (>90 %) were supplied by Sigma-Aldrich and used without further purification. For SANS and NMR measurements, deuterated SDS (96 %D in the tail to match the scattering length density of D_2O) and tail-perdeuterated SDS were synthesized at the ISIS Deuteration Facility with a 96 %D to match the scattering length density of D_2O. Similarly, deuterated DDM (51 %D in the headgroup, 89 %D in the tail) [32], and DDM with deuterated tail (89 %D) and protiated headgroup (0 %D) were prepared at the Deuteration and Macromolecular Crystallisation platform of the European Spallation Source using the literature procedure described by Midtgaard *et al.* [32].

2.2. Methods

Stock solutions of protein and surfactants were prepared in 10 mM sodium phosphate buffer at pH 7. Samples in D_2O for SANS

measurements were prepared at a pH of 7.4 to achieve a pD of 7.0, according to Rubinson's protocol [33]. All samples contained 0.01 wt% NaN_3 to avoid bacterial proliferation and were used within 72 h after preparation. Protein concentration was determined on Nanodrop 1000 (Thermo Scientific, US) using the 280 nm absorption peak.

Titration fluorescence spectroscopy (intrinsic) was performed on a Probe Drum (Labbot, Sweden) at a temperature of 25 °C. A titrant volume of 2 μL was added every minute for 100 steps (total volume added 200 μL) to a starting volume of 900 μL of titrand under continuous stirring. After 30 s equilibration, emission spectra between 215 nm and 730 nm were recorded using an excitation wavelength of 280 nm for each step. Starting titrand concentration was 67.8 μM (1.48 mg/mL) for hGH, 22.5 μM (1.49 mg/mL) for BSA, and 81.5 μM (1.48 mg/mL) for βLG. Titrant concentrations were 72 mM SDS, and 144 or 288 mM DDM for hGH, and 75 mM SDS and 300 mM DDM for BSA and βLG. For measurements starting with premixed protein and SDS, the SDS/protein ratio was selected from the initial experiments from single surfactant systems, i.e., 45 SDS/hGH, 130 SDS/BSA and 72 SDS/βLG. In addition, measurements for three different initial states were performed for hGH using SDS/hGH 15, 45 or 90.

Far-UV CD measurements were performed on a Jasco J-715 spectropolarimeter at 25 ℃. Data were acquired between 190 nm and 250 nm, using 50 nm min^{-1} scan speed, a spectral bandwidth of 1 nm, and a response time of 1 s. Each spectrum results from the accumulation of 5 scans. Protein concentration was 9.1 μM (ca. 0.21 mg mL^{-1}) for hGH, 3.1 μM (ca. 0.21 mg mL^{-1}) for BSA, and 11.4 μM (ca. 0.42 mg mL^{-1}) for βLG. Samples were loaded in a 1-mm path length quartz cuvette. The contribution from the phosphate buffer was subtracted. Data were subsequently corrected for protein concentration and number of protein residues to determine the mean residue ellipticity ($[\theta]_{MR}$) in deg cm^2 $dmol^{-1}$.

^{1}H NMR experiments were performed at the NMR center at Gothenburg University, Sweden, on a Bruker Advance III HD 800 MHz spectrometer equipped with a 5 mm TXO cold probe at 37 °C. 1D experiments were run with 126 or 128 scans, 2.045 s acquisition time, 1.5 s delay time, and 16 kHz spectral width. The protein concentration was increased to 3.5 mM (8 mg/mL) to acquire an adequate signal-to-noise ratio. Sample preparation was performed by serial dilution of stock solutions prepared in buffered D_2O. Tail-deuterated SDS was used in these experiments to minimize signal overlapping with the protein. Besides, tail-deuterated DDM was employed in the NMR experiments containing large quantities of this surfactant, i.e., those starting at 45 SDS/hGH. Surfactant concentrations used in these experiments were selected from the key transitions obtained from the titration experiment. Correlation plots, as the representation of the spectral intensities in the backbone and amide region of the spectra (6–8.5 ppm) for two different samples against each other, are included to provide a quantitative assessment of the likeness between selected spectra. As a general rule, the native spectrum is used as a baseline comparison. From these plots, the spectral similarity was parametrized using the Pearson correlation coefficient (R^2) using Matlab R2020a, which starts at 0 for two spectra with no similarity and approaches 1 as the likeness of spectra increases. In addition, ^{1}H–^{13}C SOFAST-HMQC spectra were acquired on selected samples with a ^{1}H spectral width of 13 ppm using 1040 and 256 points in direct and indirect dimension, respectively. Spectra were processed using the nmrPipe software suite [34].

SANS experiments were performed on D22 at Institut Laue-Langevin (France) and on Larmor at ISIS Pulsed Neutron Source (UK) [35,36]. Data were reduced according to standard protocols of each beamline [37,38], and instrument resolution was accounted for by smearing the theoretical models using a Gaussian function [39]. Larmor is a time-of-flight neutron instrument operated in SANS mode at fixed sample-to-detector distance of 4 m, providing a momentum transfer (q) range of 0.004–0.8 $Å^{-1}$. The sample stage was equipped with the NURF setup, allowing for in situ collection of UV–vis absorption and fluorescence emission data [40]. The spectroscopy data was used to cross-check protein concentration and correlate the interaction stage to our in-house fluorescence spectroscopy results. D22 used distances of 1.3 m

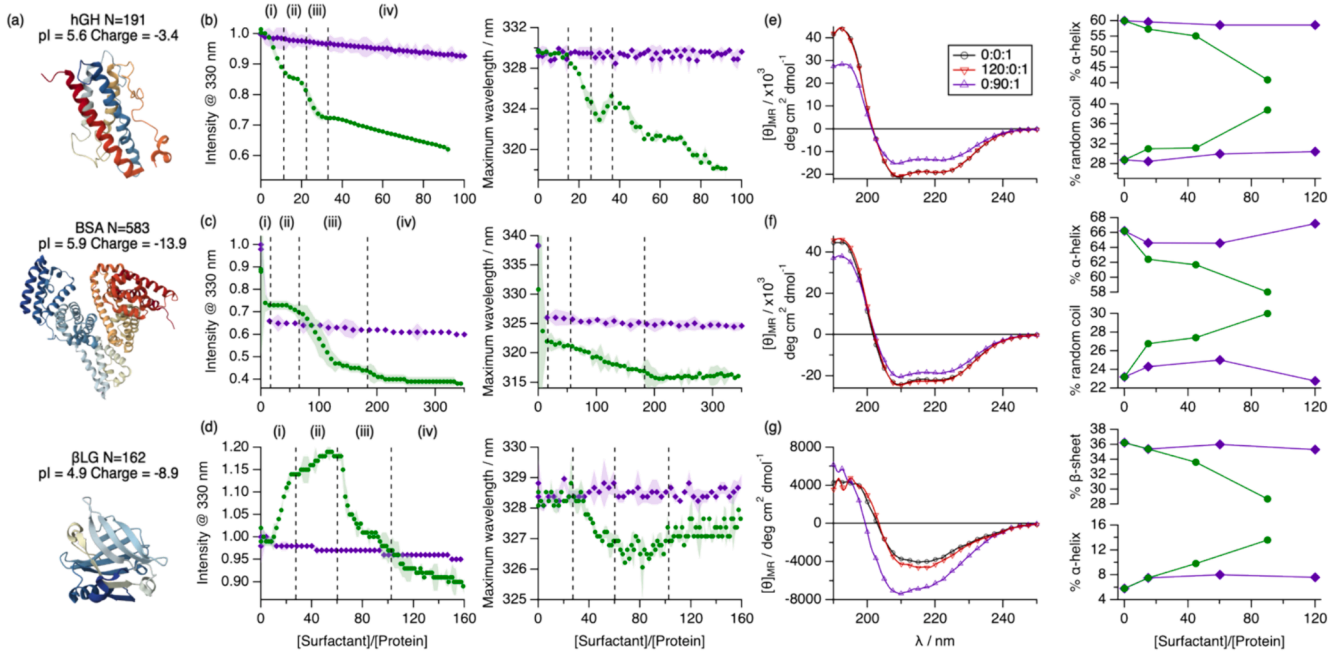

Fig. 1. (a) Monomer structure, number of amino acids (N), isoelectric point (pI), and estimated net charge at pH 7 of the native proteins: hGH – PDB entry: 3HHR [49], BSA – PDB entry: 4F5S [52], and βLG – PDB entry: 2AKQ [50]. Intrinsic fluorescence characterization of hGH (b), BSA (c), and βLG (d) during titration with DDM (◆) or SDS (●): evolution of the intensity at λ_{em} = 330 nm (normalized to the emission of the native state) and maximum peak position as a function of the surfactant-to-protein ratio. The dashed lines represent the transitions in the spectral parameters occurring upon SDS addition. Representative CD spectra and evolution of the secondary structure of hGH (e), BSA (f), mM βLG (g) in the presence of different amounts of DDM (◆) or SDS (●), as shown in (e). Secondary structure contents were calculated from the far-UV CD data using BeStSel [53]. Protein concentrations were 67.3 μM and 9.1 μM for hGH, 22.5 μM and 3.1 μM for BSA, and 81.5 μM and 11.4 μM for βLG in fluorescence and CD spectroscopy experiments, respectively, and surfactant concentrations were as indicated by the ratios.

and 8 m for the front and rear detector, respectively, giving a q-range of 0.008–0.9 $Å^{1}$. Samples were loaded in 1-mm path length quartz cuvettes and placed in a temperature-controlled sample changer. All experiments were performed using 0.154 mM hGH in D_2O, 10 mM pH 7.4 phosphate buffer solutions at 25 °C. Contrast-match experiments were performed using isotopically labelled surfactants (*vide supra*) to make the protein structure the only effective scatterer. SasView 5.0 was used for model-based fitting [41]. Structure factor deconvolution for IFT analysis was performed using the protocol previously described [27,42–44]. In brief, data were analyzed using prolate ellipsoid model to account for the protein form factor and the rescaled mean spherical approximation (RMSA) to model the structure factor contribution arising from long-range electrostatic interactions between scatterers [45,46]. Subsequently, the experimental scattering intensity was divided by the structure factor contribution to obtain a corrected scattering pattern that excludes interparticle correlations. Corrected data were analyzed using GNOM (ATSAS package) to conduct the indirect Fourier transform (IFT) method to determine the pair distance distribution function P(r) [47]. The P(r) represents a histogram of all the distances between two points within the scatterer and allows structural information of the protein to be extracted: D_{max} is the maximum dimension of the scatterer (protein), r_1 is a descriptive parameter that relates to the folding state of the protein unit (i.e., tertiary structure) and corresponds to the position of the first oscillation in the P(r), and N_{agg} parametrizes the self-association of the protein, i.e., the number of associated protein units in a single scatterer [42]. Besides, an empirical parameter that quantifies the deviation of the monomer structure from the native folding (δ value) was determined from the structural characterization.

Further details in data reduction and analysis protocols are presented in the Supporting Material.

3. Results and discussion

3.1. Surfactant synergy defines protein unfolding and refolding

To obtain an initial picture of the interaction of hGH with the individual surfactants, intrinsic emission fluorescence spectra (λ_{Ex} = 280 nm) were recorded as the nonionic DDM or anionic SDS were titrated to a protein solution. Our results systematically show that no major changes are observed in the intrinsic fluorescence emission spectra when DDM is added to the proteins (Figure S1). Only a subtle decrease in the emitted intensity at 330 nm (maximum intensity in the native state) occurs, which is attributed to a dilution effect upon titration, ca. 11 % decrease in protein concentration (Fig. 1b, c, and d). This is further confirmed by titration results with buffer (no surfactant added), as the evolution of the spectral intensities overlap (Figure S2). It should be noted that the subtle shoulder arising at 280 nm (i.e., the excitation wavelength) with increasing DDM concentration is attributed to the scattering from DDM micelles above the CMC, i.e., 0.18 mM [48]. Thus, DDM shows no interaction that affects the environment of the fluorophores excited at 280 nm of hGH and βLG, TRP and TYR, which are mainly located in the protein core [49,50]. In contrast, an initial decrease of the emitted intensity of BSA is observed, possibly attributed to the ability of this protein to bind amphipathic molecules through six high-energy binding sites without severely altering protein fold [51]. In addition, the secondary structure of the protein shows no changes in the presence of DDM, with the CD spectra overlapping at all concentration and no variations in the calculated contents. These results agree with previous reports on the resilience of compactly folded proteins to the addition of nonionic surfactants, which shows no major effects on the protein [2].

Upon SDS titration, significant alterations in the intensity, maximum peak position, and overall line shape of the intrinsic emission fluorescence spectra are observed across all proteins (Figure S1). The investigated SDS concentration range covers a premicellar state (CMC = 4.1 mM in 10 mM, pH 7 phosphate buffer), implying that the surfactant likely resides either in its monomeric form or in association with the protein [27], and thus the interaction is solely attributed to the gradual binding of individual surfactant molecules. The evolution of emission spectra follows different sequential stages. Generally, it is noted that early changes (<20 SDS molecules per protein) are more prominently reflected in alterations in emission intensity, while the emission wavelength remains relatively stable in this concentration range. For hGH and BSA (Fig. 1b, c), a sharp decrease in the intensity is initially observed at low SDS content (i). Subsequent addition of surfactant yields minimal changes in intensity (ii). A second decline in intensity occurs at intermediate SDS contents (iii), beyond which no further alterations in the spectral parameters are observed, except for the dilution effect (iv). Regarding the maximum peak position, a blue shift follows the same transitions outlined for the changes in the intensity. The absolute change in this position ranges from ca. 330 nm and 331 nm in the native state of hGH and BSA, respectively, to 318 nm and 316 nm at the highest SDS content. This is generally attributed to a more hydrophobic environment of tryptophan [54], which could be due to the presence of the SDS alkyl chains neighboring the protein chromophore. βLG exhibits analogous sequential transitions, albeit the intensity sharply evolves toward higher values during stage (i) and more subtly during stage (iii) (Fig. 1d). These changes in the intensity are accompanied by a red shift in the wavelength corresponding to the maximum emission occurs at stage (iv), unlike for the other two proteins.

These changes in the intrinsic fluorescence are associated to the interaction between the protein and the surfactant and, although the changes seem protein dependent still represent the key transitions occurring in the system. Notably, the transitions occur at different surfactant-to-protein ratios for each protein. For instance, BSA requires three times more surfactant to reach the same stage compared to hGH. This is possibly attributed to the considerably larger size of BSA, as expected from Tanford's model of surfactant-induced denaturation [55]. However, the shape of the titration curves is indicative of a strong interaction with SDS, resulting in major changes in the cybotactic environment of the protein fluorophores. Previous investigations have related these transitions to changes in the higher-order structure of proteins. For instance, hGH undergoes a sequential denaturation pathway upon SDS addition, ranging from the stabilization of a molten globule at low SDS content to the formation of a decorated micelle structure at SDS concentrations close to the CMC of the surfactant [27]. Similarly, a sequential denaturation model has been proposed for the interaction of BSA and SDS, ranging from randomly adsorbed surfactant molecules at low SDS content to the formation of more complex structures [23,26], although the architecture of the resulting complex has been subjected to debate [13].

To investigate the effects of surfactant addition in the secondary structure of the proteins, CD measurements were performed (Figure S3). The addition of DDM did not cause detectable changes in any of the three proteins, and their secondary structures remained mostly identical to the native state (Fig. 1e, f, g). In contrast, the spectra changed upon addition of SDS. For hGH and BSA, we saw a gradual reduction in the negative CD signals, mainly at 209 nm. These changes are attributed to a decrease in the ordered secondary structure domains, i.e., α-helices, accompanied by an increase of disordered regions (Fig. 1e, f). For βLG, which is predominantly populated by β-sheets, we observed a decrease in the content of β-sheet that is compensated by an increase in the amount of α-helix in the presence of SDS (Fig. 1g), as previously observed [17]. Therefore, the native populations of secondary structure motifs are strongly affected upon SDS addition for all these proteins, where highest concentrations of SDS lead to greater changes, while the protein hardly changes its structure in the presence of DDM.

Once the interactions (or lack thereof) of the individual surfactants with the proteins were determined, we focus our attention on the refolding process. This phenomenon has been previously reported as a mechanism to retrieve the native conformation of surfactant-unfolded proteins by the addition of a nonionic surfactant [17,18,22]. We

initially performed fluorescence spectroscopy titration to determine the transition points upon DDM addition. Based on the phases observed when mixing SDS and the proteins, the initial SDS concentration was selected at a ratio where significant interaction with the protein occurs, i.e., 45 SDS/hGH, 130 SDS/BSA and 72 SDS/βLG. Moreover, the system containing hGH was investigated at two additional starting ratios, i.e., 15 and 90 SDS/hGH.

With the gradual addition of DDM, the characteristic spectral features change in a non-monotonic fashion for the three proteins (Figure S4), where different stages of interaction between DDM and the SDS-protein complexes are identified (Fig. 2a, b, c). The first stage (ri) occurs at low DDM/SDS ratios and is characterized by a blue shift in the maximum emission wavelength, therefore shifting away from the value associated to the native states. At intermediate DDM/SDS rations (rii), a gradual red shift of this parameter is observed. The final stage (riii) is found above 10 DDM/SDS, where the value of the wavelength plateaus. The changes in the emission wavelength are accompanied by variations in the emitted intensity at 330 nm but those differ between the proteins. The emitted intensity from BSA slightly drops at low DDM/SDS ratios (ri) and then increases (rii), before reaching a plateau excluding the dilution effect (riii). It is hypothesized that this initial drop in intensity could be attributed to a reorganization of the surfactants at the protein envelope, possibly connected to the distinct binding ability of BSA [51]. In contrast, this drop in intensity is not observed for hGH and βLG. Instead, the intensity increases to maxima at ca. 5 DDM/SDS to then gradually decrease. Upon further addition of DDM, the transition to the last stage (riii) is observed as a change in the slope of the decay. As observed in the case of the individual surfactants, the variation in the spectral intensity between proteins is possibly associated to a different response in the proteins' higher-order structure to the interactions with the surfactants.

The transitions between the different stages are governed by the SDS/DDM ratio for a given protein, as these overlap when plotted as a function of this variable (Figure S5). Instead, the ratios change between proteins. For instance, the transitions occur at much lower SDS/DDM ratios for BSA than for hGH. This is surprising since one could expect that the larger size of BSA would shift the transitions to higher ratios, as observed for the individual surfactants. However, the changes in the higher structure of the protein could not necessarily correlate with the size of the protein, but rather with the binding affinity and structural resilience of the protein [17].

In addition, the effect of the mixing protocol was investigated to elucidate if the interactions are controlled by the equilibrium or whether initial interactions predefine the final state of the system. As such, the previous results were compared to samples where a mixture of DDM/SDS was added to hGH. The results show a practically identical fluorescence emission spectra when reaching the same DDM:SDS:hGH ratios despite the mixing protocol (Figure S6). In fact, the addition of mixed micelles with a 12 DDM/SDS ratio, where the partial recovery of the native spectral parameters was expected (Fig. 2a), did not result in protein unfolding. Thus, the mixing order does not affect the refolding process or complex formation, indicating that the system resides in a dynamic equilibrium. This was further confirmed by our stability studies, which showed that the fluorescence signal did not change over 3 days for SDS-hGH and DDM-SDS-hGH systems (Figure S7).

Therefore, the evolution of the spectral features suggests that the addition of DDM changes the environment of the protein fluorophores. Initially, the changes evolve even further away from those attributed to the native proteins, suggesting a greater degree of unfolding at low DDM contents in the presence of SDS (ri). Above a threshold concentration (rii), the trend is reversed, and the features gradually evolve toward the native state. Finally, the results indicate that the higher-order structure of the proteins is stabilized at high DDM content (riii). An important aspect is that the features of emission spectra for the native proteins are not recovered even with a large excess of DDM and that the extent of recovery differs for each protein (Fig. 2d, e, f), with hGH reaching closer values than those for BSA and βLG. As such, the results suggest that the native higher-order structure may not be fully recovered even with

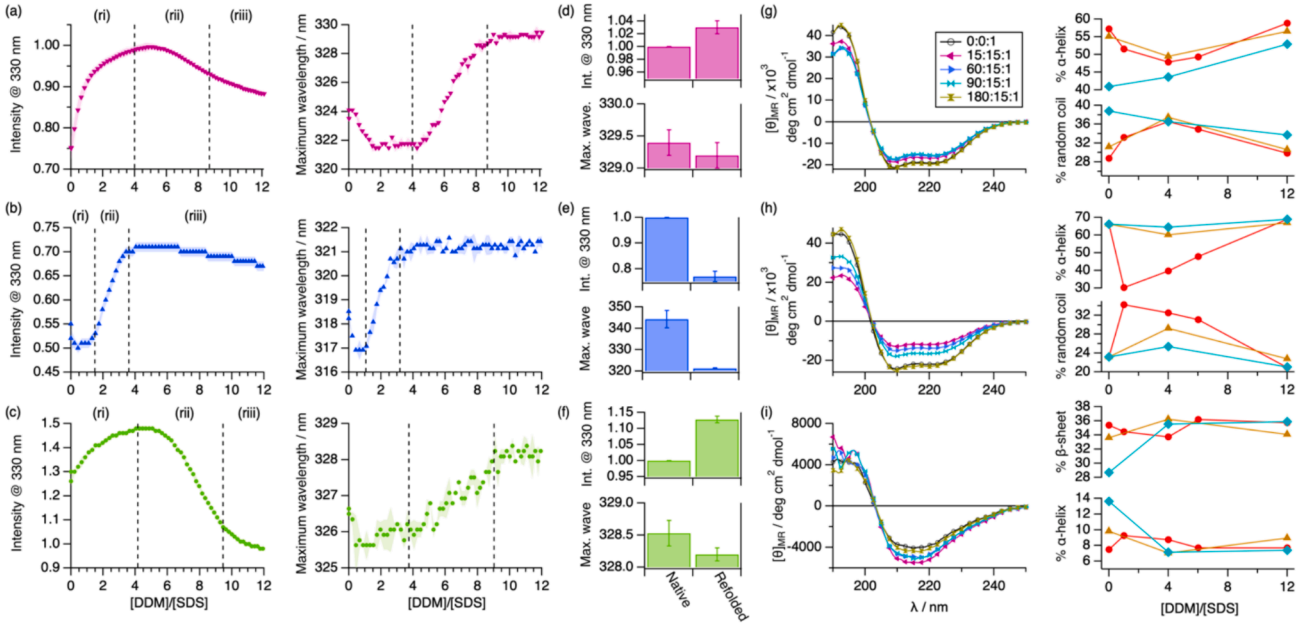

Fig. 2. Intrinsic fluorescence characterization of the addition of DDM to the SDS-unfolded proteins at an initial [SDS] = 3 mM: evolution of the intensity at λ_{em} = 330 nm (normalized to the emission of the native state) and maximum peak position as a function of the DDM-to-SDS ratio for (a) hGH, (b) BSA, and (c) βLG. The dashed lines represent the transitions in the spectral parameters occurring upon DDM addition to the SDS-unfolded proteins. Spectral features for the native and refolded state for (d) hGH, (e) BSA, and (f) βLG. Error bars (standard deviation from duplicates) are shown for all data points. Representative CD spectra and evolution of the secondary structure of hGH (g), BSA (h), mM βLG (i) at different DDM:SDS:protein ratios, as shown in the legend of graph (g). The secondary structure contents are displayed as a function of the DDM:SDS ratio for samples starting with different SDS:protein ratios 15 (●), 45 (▲), and 90 (◆). Secondary structure contents were calculated from the far-UV CD data using BeStSel [53]. Protein concentrations were 67.3 μM and 9.1 μM for hGH, 22.5 μM and 3.1 μM for BSA, and 81.5 μM and 11.4 μM for βLG in fluorescence and CD spectroscopy experiments, respectively, and surfactant concentrations were as indicated by the ratios.

exceeding concentrations of DDM.

Far-UV CD was used to determine the variations in the secondary structure of the proteins in the presence of the two surfactants (Figure S8). Interestingly, the calculated secondary structure contents demonstrate that the presence of low amounts of DDM (DDM/SDS $\leq$ 4) causes a further loss of the native secondar structure. In the case of hGH and BSA, a loss of helicity and an increase in the number of disordered regions is observed (Fig. 2g, h), whereas βLG undergoes a β-sheet-to-α-helix transition. Although these structural changes have been previously observed for BSA and βLG upon interaction with SDS [17], these results confirm the synergistic effect of SDS and DDM in the unfolding of proteins. Interestingly, the extent of synergistic unfolding is more prominent at lower SDS contents, i.e., 15 SDS/protein, while it decreases at 45 and 90 SDS/protein ratios despite maintaining the DDM/SDS ratio. As such, it is hypothesized that the interaction becomes cooperative at low SDS/protein ratios, where the proteins are possibly not saturated with surfactant molecules and SDS mediates the interaction with DDM. This saturation threshold may be the reason why the surfactant cooperation has not been previously observed, as the conditions explored so far used considerably higher SDS concentrations, e.g., 10 or 25 mM, where the proteins were possibly saturated with SDS prior DDM addition [18,25]. Upon increasing the DDM content (DDM/SDS $\geq$ 4), the contents of the secondary structure gradually evolve toward those associated to the native state, confirming that further addition of DDM prompted a gradual recovery of the proteins' secondary structure. Notably, the contents associated to the native state were fully regained (within error) for the three proteins investigated here.

Therefore, our findings highlight the differences between the behavior of surfactants whether they operate individually in a surfactant–protein system or within a ternary system comprising the two surfactants and the protein. DDM can further unfold the SDS-unfolded proteins at low SDS/protein ratios, which is not observed in the case of the native proteins. It is hypothesized that the structurally loose molten globules formed by the SDS-protein complexes could interact with DDM unlike compactly folded native proteins [12,27]. If the content of DDM is increased, a gradual recovery of the higher-order native structure of is observed. However, the results from the titration suggest that full recovery may not be achievable, although the native secondary structure of the protein is regained. Our findings also reveal that the DDM/SDS ratio is critical for modulating protein response. For example, the DDM concentration required to retrieve the spectral features similar to those of the native state of hGH scales with SDS concentration, i.e., ca. 10 DDM/SDS. Thus, a 10 mM DDM concentration is required to refold hGH in the presence of 1 mM SDS.

3.2. A model to understand surfactant-induced unfolding and refolding

With these results at hand, we sought to determine a detailed model of protein-surfactant interactions employing NMR and SANS techniques for the systems containing hGH. Initially, ^{1}H NMR measurements of native hGH and hGH in the presence of either SDS or DDM were performed to study the local environment of the protein backbone. The partial spectra covering the aromatic region (8.8–5.8 ppm) show that the overall peak pattern with and without DDM is rather similar at all surfactant concentrations investigated here (Fig. 3a). The subtle differences, consisting of a peak broadening and overall intensity loss at the highest DDM content, could be attributed to the slower tumbling of the protein in the presence of high contents of DDM. In addition, the correlation plots show a narrow distribution around the self-correlation signal (Fig. 3c). As the main features are conserved in these spectra at two different DDM contents, changes in the R^2-values are likely attributed to the broadening of the peaks (Fig. 3d). Therefore, no major transitions occur in the higher-order structure of hGH in the presence of DDM.

In contrast, the peak pattern of hGH with SDS considerably changes compared to the peaks of the native hGH sample (Fig. 3b). At 0:15:1, the peaks shift and broaden, which is possibly associated to a change in the protein backbone structure and an increase in its conformational flexibility compared to the native state. Upon increasing SDS content, i.e., 0:45:1 and 0:90:1 DDM:SDS:hGH, no major changes are observed in the position of the peaks compared to 0:15:1 DDM:SDS:hGH. However, the peaks show sharper features at higher SDS contents, suggesting that that the protein backbone presents a similar local environment, but it adopts more restricted dynamics at higher SDS content compared to the lower SDS content. These differences are confirmed by the correlation plots (Fig. 3c), with a decreasing value of the self-correlation signal with increasing SDS/hGH ratio (Fig. 3d).

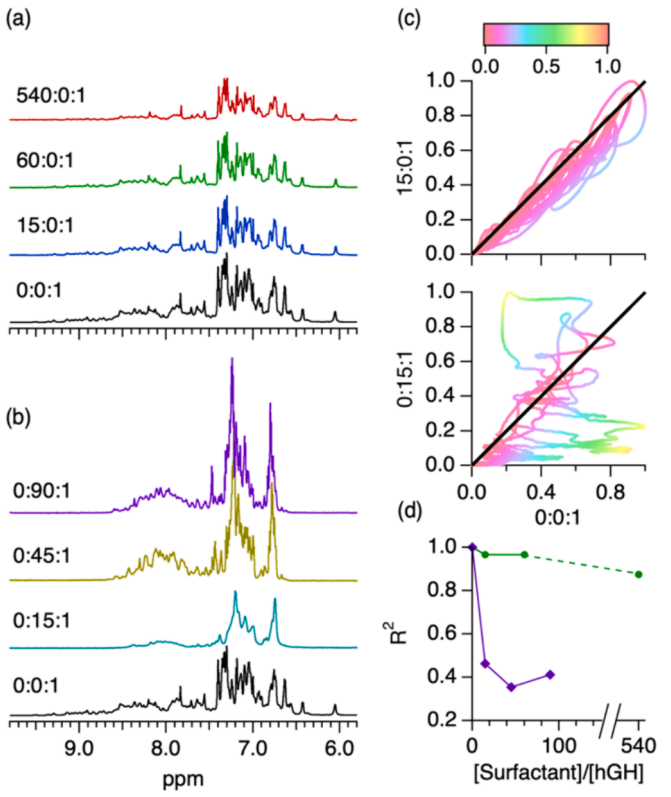

Fig. 3. ^{1}H NMR spectra of the protein backbone of 3.5 mM hGH in the absence and presence of DDM (a) and SDS (b) at selected surfactant-to-protein ratios, as indicated in the graph legends. (c) The correlation plots comparing the signal of native hGH against hGH in the presence of surfactant are shown for different surfactant-to-protein ratios for DDM (15:0:1 DDM:SDS:hGH) and SDS (0:15:1 DDM:SDS:hGH). The diagonal line in the correlation plots indicates the self-correlation of the native spectra ($R^2 = 1$) and divergence from these values is presented as a heatmap. (d) R^2-parameter derived from the analysis of the correlation plots for hGH in the presence of DDM (◆) or SDS (●).

Contrast-variation SANS was performed to probe the changes in the tertiary and quaternary structure of the protein in the presence of surfactant. The contrast-matching approach allows selective study of the structure of the protein by matching the scattering length density of the isotopically labelled surfactants to that of D_2O, which effectively makes the surfactants "invisible" to neutrons [32]. The SANS results complement the previous observations. The addition of DDM did not result in changes in the overall size, shape, and self-association of the protein at any of the investigated concentrations (Fig. 4a, c, and Table S1). In contrast, SDS significantly perturbs the structure of hGH (Fig. 4b), leading to different degrees of unfolding and, to some extent, oligomer formation (Fig. 4d). The initial addition of SDS, i.e., 0:8:1 DDM:SDS:hGH, prompts hGH to unfold (Fig. 4c, d), as judged by the shape of the P(r) and the structural parameters. While the native protein resides in a monomeric state, the addition of SDS readily prompts the oligomerization of hGH (potentially into dimers-trimers), as reflected in the

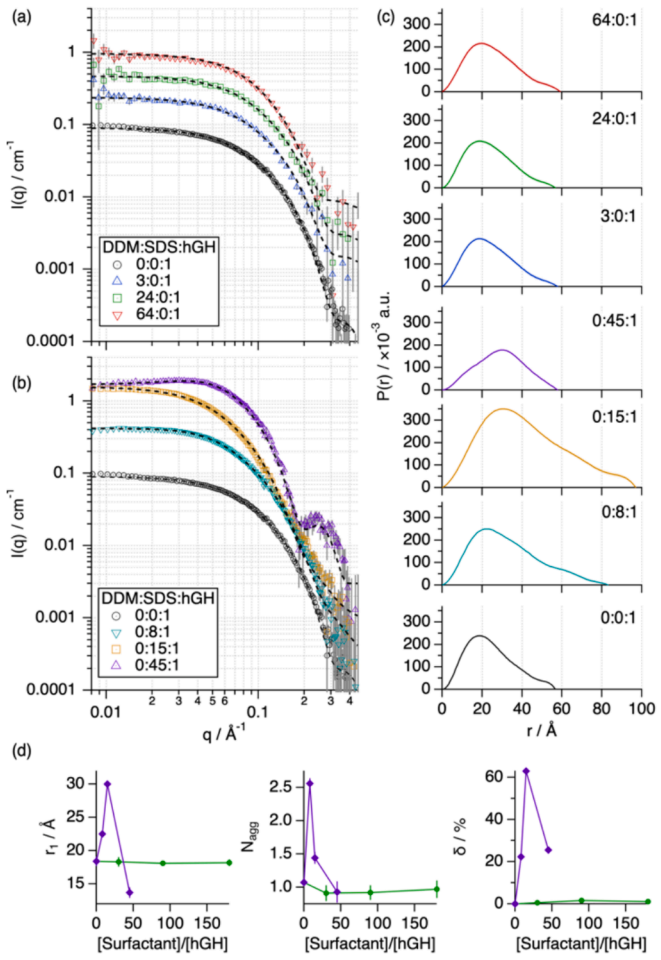

Fig. 4. Structural characterization of hGH using contrast-variation SANS. Data and best fits for 0.154 mM hGH in 10 mM phosphate buffer, pH 7.4, in D_2O in the presence of isotopically labelled (a) DDM and (b) SDS at different ratios, as indicated in the legends of the graphs. The contrast-matching approach makes the protein the only visible scatterer and the background contribution from the solvent and surfactant solutions were subtracted. The dotted lines correspond to fits obtained with the IFT method including the structure factor contribution. The SANS data and fits were scaled by a factor of × 1, ×2, ×4, and × 8 for clarity. (c) shows the P(r) associated to the data in (a) and (b). (d) Parameters derived from the analysis of the SANS data of hGH in the presence of DDM (◆) or SDS (●). Error bars (standard deviation) are shown for all data and, where not visible, the error bars are within the markers.

increased N_{agg}. These trends are gradually reversed at higher SDS content, as seen in a decrease of the characteristic dimensions and N_{agg} of the scatterer at 0:15:1 DDM:SDS:hGH. At the highest SDS content, 0:45:1 DDM:SDS:hGH, the P(r) confirm the formation of a hollow shell in terms of scattering contrast (confirmed by the oscillation centered at 0.25 q^{-1}). The analysis confirms the transition to an unfolded protein with a small characteristic distance of 13.7 Å, corresponding to the thickness of the shell [27]. These observations converge in the δ value, which shows that the addition of DDM does not cause changes in the folding state (<2%), whereas SDS profoundly affects hGH conformation.

Our characterization of the interaction of these surfactants with hGH converges in one key idea, concurring with the model developed by Otzen and co-workers [13]: DDM, as a nonionic surfactant, hardly interacts with the compactly folded hGH, while SDS significantly perturbs its higher-order structure and overall conformation in a sequential order controlled by the surfactant-to-protein ratio: first, a shift from native to a highly flexible expanded structure where the hydrophobic core expands as surfactants bind, second, a molten globule structure where the tertiary structure is disrupted leading to the exposure of hydrophobic residues, and, lastly, a transition to a decorated micelle where the protein surrounds a micelle-like surfactant assembly and the secondary structure has been (at least partially) disrupted [27]. Above this SDS content, SDS micelles begin to form in the bulk phase and only minor changes occur to the complex structure and dynamics. These different interaction stages define the conformation of the protein and the phase adopted by the surfactants attached to the protein, and undoubtedly affect its physicochemical behavior.

The spectroscopic characterization suggests that the changes induced by SDS are reversible for hGH by the subsequent addition of nonionic surfactant (Fig. 2). As such, we sought to investigate the nature of the interaction mechanism when the two surfactants are present. The local environment of the protein backbone was investigated by ^{1}H NMR measurements for selected DDM:SDS:hGH ratios. Of the possible combinations in a DDM:SDS:hGH matrix at a constant hGH concentration, two types of studies were performed: (a) samples with a constant SDS/hGH ratio at different DDM contents, and (b) samples with a constant DDM/SDS ratio at different total surfactant contents.

Shifts in the backbone proton peak pattern were studied at 15, 45, or 90 SDS/hGH, and between 1 and 12 DDM/SDS, corresponding to the regions studied by intrinsic fluorescence spectroscopy. While keeping constant hGH and SDS concentrations, shifts in the peak pattern of the protein backbone occur (Fig. 5a). When starting at 0:15:1 DDM:SDS:hGH, the addition of DDM between 1 and 4 DDM/SDS causes changes in the spectra, mainly observed in the narrowing of the peaks. These spectra further deviate from that of the native state and 0:15:1:1 DDM:SDS:hGH, particularly in the spectral features between 8.0 and 7.0 ppm, and 6.8 and 6.5 ppm. Also, a decrease in the correlation coefficient is observed (Fig. 5d and Figure S10). This transition corresponds to the regions where intrinsic fluorescence showed changes in the opposite direction to the native spectral features upon DDM addition, confirming that low quantities of the nonionic surfactant unexpectedly cause further changes in the backbone of the SDS-unfolded protein.

In contrast, when the DDM content is increased to 90:15:1 the trend is reversed and a subtle increase in the correlation coefficient is observed (Fig. 5d). At 180:15:1 DDM:SDS:hGH, the peak pattern changes again and displays very similar features to those of the native peak spectrum. Compared to the native state, the spectrum at this ratio mostly retrieves the peak positions but the features are slightly broadened, resulting in a significant recovery of the correlation signal (Fig. 5c). Particularly, the features between 8.0 and 7.0 ppm, and 6.6 and 6.0 ppm are similar to the native pattern, while the group at ca. 6.8 ppm retains the shape observed at 6 DDM/SDS. This suggests that at 180:15:1 DDM:SDS:hGH the protein backbone partially retrieves its native structure. However, the changes in the spectra suggest that subtle differences still appear compared to the protein native state.

As the DDM-to-SDS ratio is the main variable that drives the interaction with hGH, the aim was to study whether the recovery of the backbone environment can also be attained when starting from different SDS-hGH states. In the following comparisons, it must be considered that peak broadening will have an impact on the values for systems with very different total surfactant content. When comparing the influence of the total surfactant content at a constant DDM/SDS ratio of 4, i.e., 60:15:1, 180:45:1, and 360:90:1 DDM:SDS:hGH (Fig. 5b), the spectra look remarkably similar (Figure S11). This indicates that the protein backbone adopts a similar environment in the presence of the two surfactants as long as there is a constant DDM/SDS ratio. In the region where the DDM/SDS ratio leads to a partial retrieve of the native signal, i.e., 12 DDM/SDS, differences are observed between the spectra at 180:15:1 and 540:45:1 DDM:SDS:hGH and, consequently, their correlation parameters. These differences are mainly attributed to the broadening of the peak signals at higher total surfactant content. However, it is observed that the main spectral features are conserved between the two systems, e.g., those between 7.4 and 7.0 ppm. Therefore, the refolding of hGH is again achieved, although the extent of recovery cannot be accurately determined due to peak broadening.

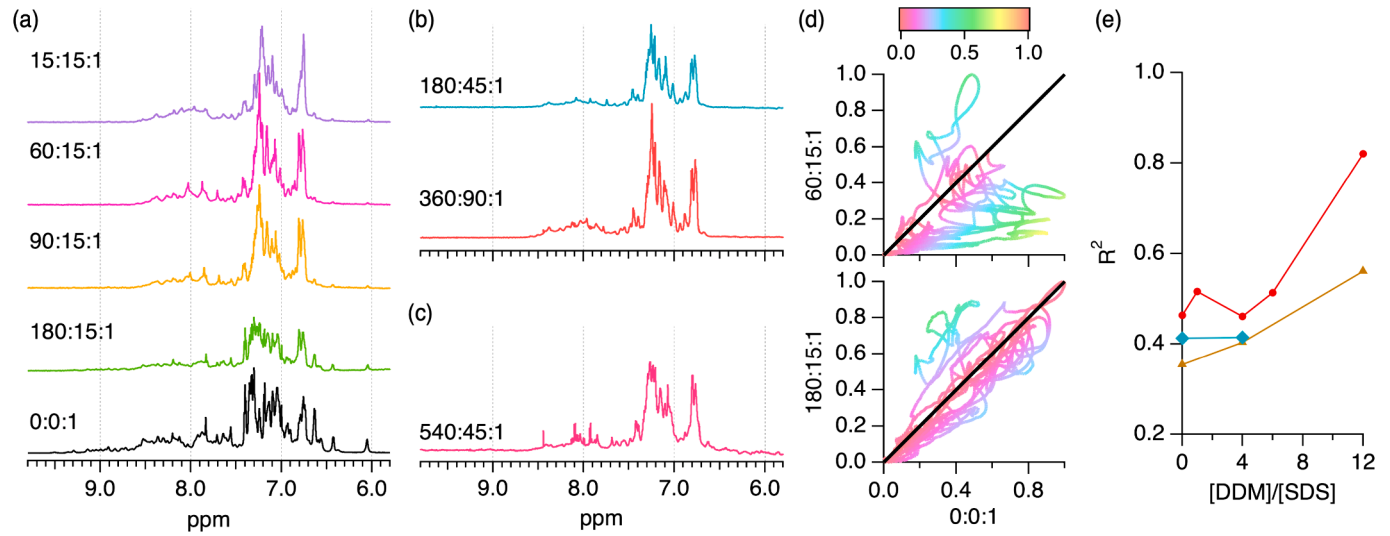

Fig. 5. ^{1}H NMR characterization of the protein backbone region for the DDM:SDS:hGH systems at 3.5 mM hGH. (a) Spectra at a constant SDS/hGH of 15 with an increasing amount of DDM. Spectra at DDM/SDS ratios of 4 (b) and 12 (c) varying the amount of SDS in the system. The ratios are indicated in the legend of the graphs. The correlation plots comparing selected spectra against the native spectrum are presented in (d). The diagonal line in the correlation plots indicates the self-correlation of the native spectra ($R^2 = 1$) and divergence from these values is presented as a heatmap. (f) displays the evolution of the parameter R^2 with varying the DMM content in the system at different initial SDS/hGH ratios: 15 (●), 45 (▲), and 90 (◆) SDS/hGH.

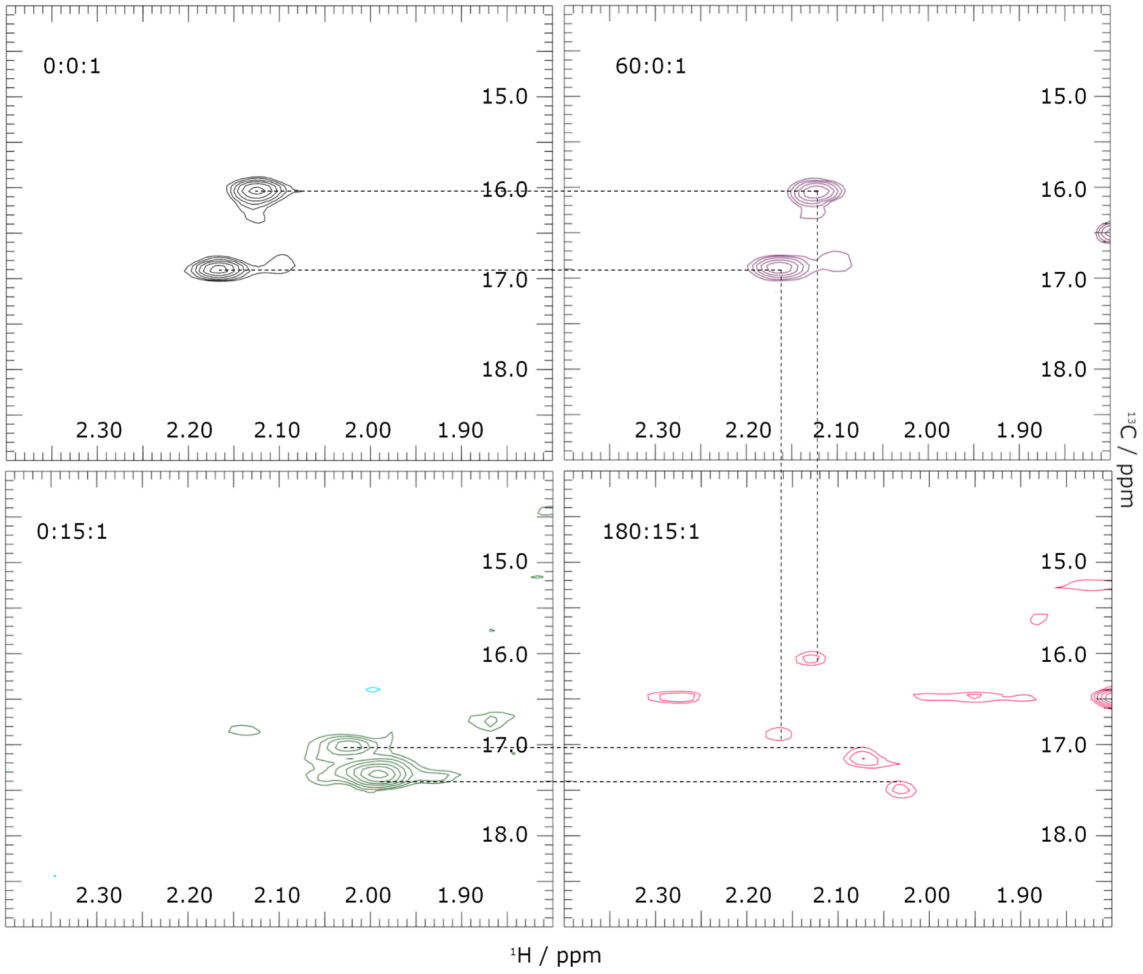

Fig. 6. 2D ^{1}H–^{13}C HMQC spectra of the protein methionine region for the DDM:SDS:hGH systems at 3.5 mM hGH. The ratios are indicated in the legend of the graphs. The dashed lines indicate the overlap between the spectra.

By looking at the evolution of the R^2-values as a function of DDM:SDS:hGH ratio some relevant aspects can be inferred (Fig. 5d). (a) The addition of low quantities of DDM to a previously SDS-unfolded hGH does not contribute to retrieving the native environment of the protein backbone and even displaces the features further away from the native state. (b) When 12 DDM/SDS is reached, the R^2-values significantly increase compared to those at lower DDM content, suggesting that the protein has retrieved, at least partially, its native higher-order structure.

To further investigate the extent of protein recovery, $^{1}H–^{13}C$ HMQC spectra were acquired on selected samples (Fig. 6). Samples with high levels of detergent show significant overlap between the signals of the surfactants and the protein, which hides the protein methyl groups. Therefore, analysis was focused primarily on the methionine side chains, which are displaced from the center of the methyl spectra [56]. Initially, the signal from the native protein was compared with experimental signal of the protein in the presence of the individual surfactants. The results clearly show an almost perfect overlay in the case of DDM (60:0:1), while the presence of SDS (0:15:1) completely suppresses the native peaks (ca. ^{1}H 2.10–2.15 ppm, ^{13}C 16.0–17.0 ppm) and new features appear in the spectra (ca. ^{1}H 1.95–2.05 ppm, ^{13}C 17.0–17.5 ppm). As expected, this correlates with the loss of the protein conformation in the presence of the anionic surfactant [27], whereas the nonionic hardly perturbs the hGH native fold. When the two surfactants are present at 12 DDM/SDS, where refolding is expected, it is observed that the spectra show both the peaks from the native conformation and a subtle signal from the characteristic SDS-unfolded hGH. In addition, new features appear in the spectra (ca. ^{1}H 2.25–2.30 ppm, ^{13}C 16.0 ppm) that could be attributed to contributions from the surfactants. However, the overlap between the native and SDS-unfolded signals in the spectra at 180:15:1 suggests the co-existence of (at least) two conformational states. It is here hypothesized that these are closely related in terms of backbone structure and these results confirm that higher-order structure of hGH cannot be fully refolded through the addition of DDM.

The influence of the interactions between the protein and the two surfactants from a conformational point of view was investigated using contrast-variation SANS (Fig. 7a, b). When starting from SDS-hGH complexes, the addition of DDM between 1 and 6 DDM/SDS causes an increase in the dimensions of the protein, either r_1 or N_{agg} (Fig. 7d). This confirms that DDM contributes to further unfolding of hGH compared to the initial SDS-unfolded state. Particularly, at 90:45:1 DDM:SDS:hGH we observed the largest deviation from the conformation in the native state, with a 1.7-fold increase in the size of the hGH monomer. In addition, the presence of DDM seems to modulate the self-association of the protein. This is possibly attributed to a re-distribution of the charge density at the surfactant–protein complex, leading to hindered electrostatic repulsion. At 180:15:1 DDM:SDS:hGH (12 DDM/SDS), the conformation of hGH is similar to the native protein (Fig. 7b, c), but some structural differences are observed. In particular, the protein recovers its monomeric state, but the characteristic size of the monomer is 1.2-fold larger than that of native hGH (Fig. 7d). Although these differences may seem relatively small, they are consistent with our NMR and could be attributed to co-existing conformational states that are closely related in terms of structure. The unfolding-refolding sequential process upon increasing DDM content can be seen in the evolution of the δ parameter (see Fig. 6c), which clearly shows a general deviation of the monomer structure at low DDM/SDS ratios before the recovery attained at high DDM/SDS ratios.

As a general picture drawn from our integrative characterization, the results demonstrates that the nonionic-to-ionic surfactant ratio controls the unfolding and refolding processes of hGH. When hGH is unfolded in the presence of SDS, the addition of small amounts of DDM (DDM/SDS between 1 and 4) promotes further protein unfolding (ri), characterized by changes in the backbone environment and a loss of the conformation of the protein. These findings contrast with the evidence that DDM does not interact with the folded state of hGH. When the DDM/SDS ratio is increased between 6 and 10, the system begins to retrieve the native fold

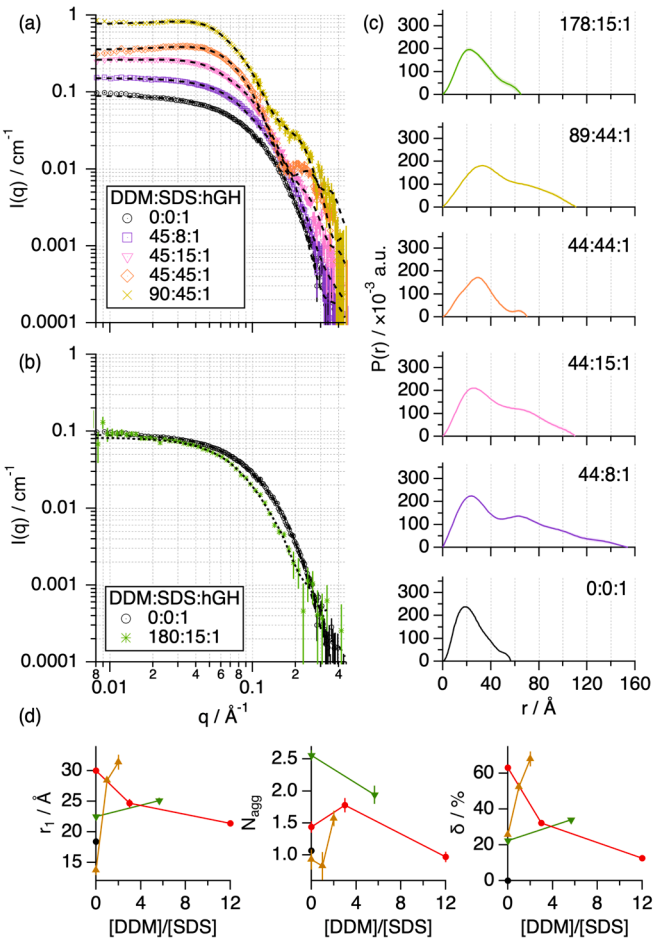

Fig. 7. Structural characterization of hGH using contrast-variation SANS. (a) and (b) Data and best fits for 0.135 mM hGH in 10 mM phosphate buffer pH = 7.4 in D_2O in the presence of isotopically labelled SDS and DDM at different ratios, as indicated in the legends of the graphs. The contrast-matching approach makes the protein the only visible scatterer and the background contribution from the solvent and surfactant solutions were subtracted. The dotted lines correspond to fits obtained with the IFT method including the structure factor contribution. The SANS data and fits in (a) were scaled by a factor of × 1, ×2, ×4, ×8, and × 16 for clarity. (c) shows the pair distance-distribution functions, P(r), associated to the data in (a) and (b). (d) Parameters derived from the analysis of the SANS data of the SDS-unfolded hGH in the presence of DDM at different starting SDS/hGH ratios: 0 (●), 8 (▼), 15 (●), and 45 (▲). The structural parameters derived from the δ as a function of DDM/SDS ratio for different starting conditions is presented in (d). Error bars (standard deviation) are shown for all data and, where not visible, the error bars are within the markers.

(rii). This transition has been finely characterized using fluorescence titration, showing a gradual recovery of the spectral features. Further increasing the DDM/SDS above 10 (riii), the protein has mostly recovered the characteristic features of the native state, that is, chromophore environment, secondary structure, backbone environment, and conformation. However, our results demonstrate that a multimodal system appears, potentially containing closely related conformations in terms of structure and dynamics, that are close but not identical to the native state of the protein.

3.3. *A general mechanism to decipher surfactant cooperation*

As demonstrated in this work, interactions between proteins and the surfactants consist of a sequence of equilibria in a dynamic landscape. The transitions between the different states can be controlled by the

surfactant ratios, and mapping the ternary system, i.e., protein, ionic surfactant, and nonionic surfactant, enables the regulation of the conformational landscape of the protein, even allowing to access a greater variety of states compared to the binary systems. To understand the full picture, these different states were investigated, covering possible unfolding and refolding pathways, as well as surfactant cooperation.

One of the key aspects demonstrated is the ability of small quantities of DDM to interact with SDS-unfolded proteins at low total surfactant content (ri). The current paradigm dictates that SDS constitutes a strongly interacting surfactant that leads to protein unfolding upon complexation, while DDM hardly affects the conformation of compactly folded proteins [13]. However, our results reveal a new interaction mechanism, that is, the nonionic surfactant can interact with partially unfolded proteins as mediated by the presence of SDS. This is possibly due to the stabilization of a highly dynamic, partially open protein structure, such as a molten globule [27], which enables the co-adsorption of DDM and SDS molecules onto the protein. Such a scenario seems plausible since hindrance would diminish due to protein unfolding, mimicking the mechanism observed for α-lactalbumin, which resides in a highly dynamic, partially folded state [12]. Also, the accretion of nonionic surfactants would reduce local electrostatic repulsion between neighboring ionic surfactants [13], thus adopting a more energetically favorable state. Notably, this effect seems to be more significant for the lower starting SDS/protein ratios, possibly as the SDS-protein complex is not yet saturated with the anionic surfactant.

On the other end of the nonionic surfactant content, at high nonionic-to-ionic surfactant ratio (riii), we find the ability of DDM to refold SDS-unfolded proteins [17]. When sufficient DDM is present in a micellar form, SDS and DDM molecules desorb from the protein complex, and the protein begins to retrieve a folded conformation. However, even at the highest DDM/SDS ratio measured here, our results suggest that the environment of the backbone and conformation of the protein cannot be fully retrieved. A close-to-native state was observed in our studies, with possibly a few surfactant molecules still adsorbed to the protein. Besides, a detailed study of the protein backbone suggests that, at this stage, the protein co-exists in different conformations that are structurally similar.

Thus, a question remains open: can a protein be fully stripped of SDS and is this a protein-dependent scenario? The characterization by fluorescence spectroscopy shows that the extent of recovery of the native spectral features differs for each protein. For instance, hGH features are recovered to a greater extent than those for BSA. This could be attributed to the recognized ability of BSA to selectively bind aliphatic moieties [51]. Therefore, it seems plausible that different proteins react differently to the surfactant-mediated protein refolding. The challenge then becomes to detect those remnant surfactant molecules associated to the protein. Previous investigations have shown that the adsorption of very few SDS molecules causes minor changes in the protein that could not be easily detected by conventional in-house methods (e.g., circular dichroism and fluorescence spectroscopy) [27]. Therefore, the surfactant-mediated refolding is likely a protein-specific process since each protein will expose different amphiphilic interfaces in the presence of surfactants. As such, future investigations shall be performed to primarily focus on studying, possibly involving advanced characterization methods, protein behavior upon refolding, where it is hypothesized that these closely related conformations co-exist in a dynamic and rapidly interchanging landscape.

Our study suggests that the cooperativity between the two surfactants constitutes the mechanistic origin of the unfolding and refolding processes in the three-component system. This brings us to hypothesize the formation of hybrid SDS and DDM nanoscale domains, either as co-assembled adsorbates in the protein complex (synergistic unfolding) or in mixed micelles at the bulk phase (refolding) [57]. For the former scenario, the co-adsorption of both surfactants onto the protein only happens in a narrow and well-defined window of nonionic-to-anionic surfactant ratio. This phenomenon is facilitated by the unfolded state of the protein and possibly mediated by the formation of SDS-hydrophobic domains [27], where the co-adsorption of DDM could be thermodynamically favored [58]. In contrast, when sufficient DDM is present in the system, the population of nonionic micelles in the bulk prompts the accretion of weakly protein-bound SDS molecules into mixed micelles [13]. Previous investigations have shown the nonideal behavior of SDS and DDM, where attractive interactions between these two surfactants are attributed to the reduction of local electrostatic repulsions between SDS molecules [57]. In such a scenario, the SDS-protein complex would favorably adsorb nonionic surfactant at low DDM concentrations, ultimately causing the synergistic unfolding of the protein. Further addition of DDM provides enough micelles (protein-free) to displace the protein-adsorbed surfactants to the micellar phase. Such an effect will cause the refolding of the protein, given that enough DDM is present in the system. From the fluorescence titration, the refolding process begins at ca. 6 DDM/SDS, which corresponds to 7 mM total surfactant concentration. This concentration is well above the CMC of DDM alone (0.18 mM) and that of DDM-SDS micelles at equimolar amounts (0.20 mM) [48,57]. Comparing this interaction to a polyelectrolyte system without a defined intramolecular folding, it has been shown that: (i) synergistic binding of DDM and SDS to the polyion occurs at a low surfactant content, and (iii) when mixed micelles are in excess the binding between SDS and the polyion can be completely suppressed [59]. Therefore, a threshold population of micelles must be required to initiate the refolding process, at a point where surfactant monomers [57], free micelles [58], and surfactant–protein complexes co-exist.

We have also shown that the structures formed here are equilibrium states, and specific conformational populations only occur in narrow ranges of DDM/SDS ratios. Experimental evidence based on NMR and SANS data shows that the synergistically unfolded state is different from that driven by SDS alone. Also, the results suggest that multiple conformational states could co-exist upon refolding. This has been previously observed as the refolding of β-lactoglobulin in a mixed surfactant system is a heterogenous process where several protein species coexist [18]. Although the protein-surfactant complexes during synergistic unfolding/refolding processes are in equilibrium with the micellar phase, the underlying mechanism behind surfactant desorption is yet to be determined. As such, future investigations shall be oriented to determine the molecular origin of those effects, possibly requiring the combination of experimental and computational methods.

4. Conclusions

In summary, we have demonstrated that the higher-order structure of proteins can be modulated through the cooperation of an anionic surfactant, SDS, and a nonionic surfactant, DDM. At low SDS content, the native conformation of the protein is disrupted, opening interaction sites for DDM to bind to the protein that was not present in the native state, and causing further unfolding. When the content of DDM is further increased, the SDS-unfolded protein gradually retrieves a compact conformation, confirming the reversibility of SDS-binding to the protein [13]. However, the native fold cannot be fully recovered even at the highest DDM-to-SDS ratios, where multiple conformational states co-exist. This mechanism can possibly be a general scenario for globular proteins, as it has been shown that the cooperation arises from the affinity between amphiphiles to associate around charged polyionic domains [59], and the affinity of nonionic surfactants for loosely folded molten globules [12]. Our results show that the ratio between the surfactants is critical for the defining the interaction stage, where the conformation of the protein evolves through a non-monotonic landscape of equilibria with increasing the DDM/SDS ratio.

To the best of our knowledge, this study is the first demonstration of surfactant cooperativity for protein unfolding. These findings are an important contribution to achieving a better understanding of protein refolding mediated by the addition of a nonionic surfactant, opening

new possibilities in the development of new formulation technologies, where the cooperative binding can be utilized for the stabilization of non-native protein folds. For instance, liquid pharmaceutical formulations could use this concept of cooperativity to enhance the colloidal stability of biologics, since the SDS-protein complexes are highly stable [27], where the folded state can be retrieved upon the addition of the third component. Also, the refolding strategy could enhance the pH resilience of the protein [11], contributing to stabilizing the system in conditions near the isoelectric point of the protein and improving protein performance in, e.g., detergency and cosmetics. Overall, our study confirms the complex interplay between proteins and surfactants can provide new routes for controlling protein conformation, opening a wide range of possibilities to be exploited in fundamental and applied investigations.

CRediT authorship contribution statement

Johanna Hjalte: Writing – original draft, Methodology, Investigation, Formal analysis. **Carl Diehl:** Writing – review & editing, Investigation, Formal analysis, Data curation. **Anna E. Leung:** Writing – review & editing, Resources, Investigation. **Jia-Fei Poon:** Writing – review & editing, Resources, Investigation. **Lionel Porcar:** Writing – review & editing, Resources, Methodology, Data curation. **Rob Dalgliesh:** Writing – review & editing, Resources, Investigation, Data curation. **Helen Sjögren:** Writing – review & editing, Supervision, Resources, Methodology, Funding acquisition. **Marie Wahlgren:** Writing – review & editing, Supervision, Project administration, Methodology, Investigation, Funding acquisition. **Adrian Sanchez-Fernandez:** Writing – review & editing, Supervision, Methodology, Investigation, Formal analysis, Conceptualization.

Declaration of competing interest

The authors declare the following financial interests/personal relationships which may be considered as potential competing interests: [Adrian Sanchez-Fernandez reports financial support was provided by Sweden's Innovation Agency. If there are other authors, they declare that they have no known competing financial interests or personal relationships that could have appeared to influence the work reported in this paper.].

Data availability

Data will be made publicly available in the Zenodo repository upon publication

Acknowledgements

The research in this study was performed with national support from Vinnova – Swedish Governmental Agency for Innovation Systems within the NextBioForm Competence Centre. Part of this work is based upon experiments performed on the Larmor instrument at the ISIS Neutron and Muon Source, Harwell (UK), and on the D22 instrument at the Institut Laue-Langevin (ILL), Grenoble (France) (experiment numbers: ISIS – RB2010630; ILL – 9-13-948) [60,61]. Also, the authors thank the Swedish NMR Centre for instrument access and help with the experimental setup. The deuterated DDM samples were synthesized by the DEMAX platform at the European Spallation Source ERIC as a result of proposal YGZX8PCG. The persistent identifier for the samples is doi: 10.5281/zenodo.3496941. The authors gratefully acknowledge the Partnership for Soft Condensed Matter (PSCM) for providing access to the laboratories. This work benefited from the use of the SasView application, originally developed under NSF award DMR-0520547. SasView contains code developed with funding from the European Union's Horizon 2020 research and innovation programme under the SINE2020 project, grant agreement no 654000.

Appendix A. Supplementary material

Supplementary data to this article can be found online at https://doi.org/10.1016/j.jcis.2024.05.157.

References

[1] V. Corradi, B.I. Sejdiu, H. Mesa-Galloso, H. Abdizadeh, S.Y. Noskov, S.J. Marrink, D.P. Tieleman, Emerging diversity in lipid-protein interactions, ChemRev 119 (9) (2019) 5775–5848.
[2] D.E. Otzen, Proteins in a brave new surfactant world, Current Opin Colloid Interf Sci 20 (3) (2015) 161–169.
[3] H.S. Olsen, P. Falholt, The role of enzymes in modern detergency, J. Surfactant Deterg. 1 (4) (1998) 555–567.
[4] M.C. Manning, D.K. Chou, B.M. Murphy, R.W. Payne, D.S. Katayama, Stability of protein pharmaceuticals: an update, Pharm. Res. 27 (4) (2010) 544–575.
[5] A.L. Shapiro, E. Viñuela, J.V. Maizel, Molecular weight estimation of polypeptide chains by electrophoresis in SDS-polyacrylamide gels, Biochem. Biophys. Res. Commun. 28 (5) (1967) 815–820.
[6] D. Otzen, Protein-surfactant interactions: a tale of many states, BBA 1814 (5) (2011) 562–591.
[7] M.L. Anson, The denaturation of proteins by detergents and bile salts, Science 90 (2333) (1939) 256–257.
[8] J.A. Reynolds, C. Tanford, The gross conformation of protein-sodium dodecyl sulfate complexes, J. Biol. Chem. 245 (1970) 5161–5165.
[9] N.B. Bam, J.L. Cleland, T.W. Randolph, Molten globule intermediate of recombinant human growth hormone: stabilization with surfactants, Biotechnol. Prog. 12 (6) (1996) 801–809.
[10] D.E. Otzen, Protein unfolding in detergents: effect of micelle structure, ionic strength, pH, and temperature, Biophys. J. 83 (4) (2002) 2219–2230.
[11] H.O. Rasmussen, D.T.W. Wollenberg, H. Wang, K.K. Andersen, C.L.P. Oliveira, C. I. Jorgensen, T.J.D. Jorgensen, D.E. Otzen, J.S. Pedersen, The changing face of SDS denaturation: complexes of thermomyces lanuginosus lipase with SDS at pH 4.0, 6.0 and 8.0, J. Colloid Interface Sci. 614 (2022) 214–232.
[12] D.E. Otzen, P. Sehgal, P. Westh, Alpha-Lactalbumin is unfolded by all classes of surfactants but by different mechanisms, J. Colloid Interface Sci. 329 (2) (2009) 273–283.
[13] D.E. Otzen, J.N. Pedersen, H.O. Rasmussen, J.S. Pedersen, How do surfactants unfold and refold proteins? Adv. Colloid Interface Sci. 308 (2022) 102754.
[14] A.H. Poghosyan, N.P. Schafer, J. Lyngso, A.A. Shahinyan, J.S. Pedersen, D. E. Otzen, Molecular dynamics study of ACBP denaturation in alkyl sulfates demonstrates possible pathways of unfolding through fused surfactant clusters, Protein Eng. Des. Sel. 32 (4) (2019) 175–190.
[15] J. Nedergaard Pedersen, P. Frederix, J. Skov Pedersen, S.J. Marrink, D.E. Otzen, Role of charge and hydrophobicity in liprotide formation: a molecular dynamics study with experimental constraints, Chembiochem 19 (3) (2018) 263–271.
[16] G. Scanavachi, Y.R. Espinosa, J.S. Yoneda, R. Rial, J.M. Ruso, R. Itri, Aggregation features of partially unfolded bovine serum albumin modulated by hydrogenated and fluorinated surfactants: molecular dynamics insights and experimental approaches, J. Colloid Interface Sci. 572 (2020) 9–21.
[17] J.D. Kaspersen, A. Sondergaard, D.J. Madsen, D.E. Otzen, J.S. Pedersen, Refolding of SDS-unfolded proteins by nonionic surfactants, Biophys. J . 112 (8) (2017) 1609–1620.
[18] J.N. Pedersen, J. Lyngso, T. Zinn, D.E. Otzen, J.S. Pedersen, A complete picture of protein unfolding and refolding in surfactants, Chem. Sci. 11 (3) (2019) 699–712.
[19] L. Buscajoni, M.C. Martinetz, M. Berkemeyer, C. Brocard, Refolding in the modern biopharmaceutical industry, Biotechnol. Adv. 61 (2022) 108050.
[20] P. Singhvi, A. Saneja, R. Ahuja, A.K. Panda, Solubilization and refolding of variety of inclusion body proteins using a novel formulation, Int. J. Biol. Macromol. 193 (Pt B) (2021) 2352–2364.
[21] T. Nojima, T. Iyoda, Egg white-based strong hydrogel via ordered protein condensation, NPG Asia Mater. 10 (1) (2018) e460–e.
[22] D. Saha, D. Ray, J. Kohlbrecher, V.K. Aswal, Unfolding and refolding of protein by a combination of ionic and nonionic surfactants, ACS Omega 3 (7) (2018) 8260–8270.
[23] S. Mehan, V.K. Aswal, J. Kohlbrecher, Tuning of protein-surfactant interaction to modify the resultant structure, Phys. Rev. E 92 (3) (2015) 032713.
[24] R.-C. Lu, J.-X. Xiao, A.-N. Cao, L.-H. Lai, B.-Y. Zhu, G.-X. Zhao, Surfactant-induced refolding of lysozyme, Biochim. Biophys. Acta Gen. Subj. 1722 (3) (2005) 271–281.
[25] H.Ø. Rasmussen, J.J. Enghild, D.E. Otzen, J.S. Pedersen, Unfolding and partial refolding of a cellulase from the SDS-denatured state: from β-sheet to α-helix and back, Biochim. Biophys. Acta Gen. Subj. 1864 (1) (2020) 129434.
[26] T. Chakraborty, I. Chakraborty, S.P. Moulik, S. Ghosh, Physicochemical and conformational studies on BSA−surfactant interaction in aqueous medium, Langmuir 25 (5) (2009) 3062–3074.
[27] A. Sanchez-Fernandez, C. Diehl, J.E. Houston, A.E. Leung, J.P. Tellam, S.E. Rogers, S. Prevost, S. Ulvenlund, H. Sjogren, M. Wahlgren, An integrative toolbox to unlock the structure and dynamics of protein-surfactant complexes, Nanoscale Adv 2 (9) (2020) 4011–4023.
[28] J.G. Hansted, P.L. Wejse, H. Bertelsen, D.E. Otzen, Effect of protein-surfactant interactions on aggregation of beta-lactoglobulin, BBA 1814 (5) (2011) 713–723.

[29] S. Ghosh, A. Banerjee, A multitechnique approach in protein/surfactant interaction study: physicochemical aspects of sodium dodecyl sulfate in the presence of trypsin in aqueous medium, Biomacromolecules 3 (1) (2002) 9–16.
[30] K. Takeda, Y. Moriyama, Comment on the misunderstanding of the BSA−SDS complex model: concern about publications of an impractical model, J. Phys. Chem. B 111 (5) (2007) 1244.
[31] K. Tejaswi Naidu, N. Prakash Prabhu, Protein-Surfactant Interaction: Sodium Dodecyl Sulfate-Induced Unfolding of Ribonuclease A, J. Phys. Chem. B 115 (49) (2011) 14760–14767.
[32] S.R. Midtgaard, T.A. Darwish, M.C. Pedersen, P. Huda, A.H. Larsen, G.V. Jensen, S. A.R. Kynde, N. Skar-Gislinge, A.J.Z. Nielsen, C. Olesen, M. Blaise, J.J. Dorosz, T. S. Thorsen, R. Venskutonyte, C. Krintel, J.V. Moller, H. Frielinghaus, E.P. Gilbert, A. Martel, J.S. Kastrup, P.E. Jensen, P. Nissen, L. Arleth, Invisible detergents for structure determination of membrane proteins by small-angle neutron scattering, FEBS J. 285 (2) (2018) 357–371.
[33] K.A. Rubinson, Practical corrections for p(H, D) measurements in mixed H2O/D2O biological buffers, Anal. Methods 9 (18) (2017) 2744–2750.
[34] F. Delaglio, S. Grzesiek, G.W. Vuister, G. Zhu, J. Pfeifer, A. Bax, NMRPipe: a multidimensional spectral processing system based on UNIX pipes, J. Biomol. NMR 6 (3) (1995) 277–293.
[35] R.K. Heenan, S.E. Rogers, D. Turner, A.E. Terry, J. Treadgold, S.M. King, Small angle neutron scattering using Sans2d, Neutron News 22 (2) (2011) 19–21.
[36] K. Lieutenant, P. Lindner, R. Gahler, A new design for the standard pinhole small-angle neutron scattering instrument D11, J. Appl. Cryst. 40 (6) (2007) 1056–1063.
[37] O. Arnold, J.C. Bilheux, J.M. Borreguero, A. Buts, S.I. Campbell, L. Chapon, M. Doucet, N. Draper, R. Ferraz Leal, M.A. Gigg, V.E. Lynch, A. Markvardsen, D. J. Mikkelson, R.L. Mikkelson, R. Miller, K. Palmen, P. Parker, G. Passos, T. G. Perring, P.F. Peterson, S. Ren, M.A. Reuter, A.T. Savici, J.W. Taylor, R.J. Taylor, R. Tolchenov, W. Zhou, J. Zikovsky, Mantid—Data analysis and visualization package for neutron scattering and μ SR experiments, Nucl. Instrum. Methods Phys. Res., Sect. A 764 (2014) 156–166.
[38] C.D. Dewhurst, Graphical reduction and analysis small-angle neutron scattering program: GRASP, J. Appl. Cryst. 56 (Pt 5) (2023) 1595–1609.
[39] J. Barker, J. Pedersen, Instrumental smearing effects in radially symmetric small-angle neutron scattering by numerical and analytical methods, J. Appl. Cryst. 28 (2) (1995) 105–114.
[40] C. Dicko, A. Engberg, J.E. Houston, A.J. Jackson, A. Pettersson, R.M. Dalgliesh, F. A. Akeroyd, D.A. Venero, S.E. Rogers, A. Martel, L. Porcar, A.R. Rennie, NUrF-Optimization of in situ UV-vis and fluorescence and autonomous characterization techniques with small-angle neutron scattering instrumentation, Rev. Sci. Instrum. 91 (7) (2020) 075111.
[41] M. Doucet, J.H. Cho, G. Alina, Z. Attala, J. Bakker, W. Bouwman, P. Butler, K. Campbell, T. Cooper-Benun, C. Durniak, L. Forster, M. Gonzales, R. Heenan, A. Jackson, S. King, P. Kienzle, J. Krzywon, T. Nielsen, L. O'Driscoll, W. Potrzebowski, S. Prescott, R. Ferraz Leal, P. Rozycko, T. Snow, A. Washington, SasView version 5.0.3, 2020. https://zenodo.org/record/3930098. Accessed 2020-08-24.
[42] A. Sanchez-Fernandez, M. Basic, J. Xiang, S. Prevost, A.J. Jackson, C. Dicko, Hydration in deep eutectic solvents induces non-monotonic changes in the conformation and stability of proteins, J. Am. Chem. Soc. 144 (51) (2022) 23657–23667.
[43] A. Sanchez-Fernandez, S. Prevost, M. Wahlgren, Deep eutectic solvents for the preservation of concentrated proteins: the case of lysozyme in 1: 2 choline chloride : glycerol, Green Chem. 24 (11) (2022) 4437–4442.
[44] A. Sanchez-Fernandez, A.J. Jackson, S.F. Prevost, J.J. Doutch, K.J. Edler, Long-Range Electrostatic Colloidal Interactions and Specific Ion Effects in Deep Eutectic Solvents, J. Am. Chem. Soc. 143 (35) (2021) 14158–14168.
[45] J.-P. Hansen, J.B. Hayter, A rescaled MSA structure factor for dilute charged colloidal dispersions, Mol. Phys. 46 (3) (2006) 651–656.
[46] J.S. Pedersen, Analysis of small-angle scattering data from colloids and polymer solutions: modeling and least-squares fitting, Adv. Colloid Interface Sci. 70 (1997) 171–210.
[47] K. Manalastas-Cantos, P.V. Konarev, N.R. Hajizadeh, A.G. Kikhney, M. V. Petoukhov, D.S. Molodenskiy, A. Panjkovich, H.D.T. Mertens, A. Gruzinov, C. Borges, C.M. Jeffries, D.I. Svergun, D. Franke, ATSAS 3.0: expanded functionality and new tools for small-angle scattering data analysis, J. Appl. Cryst. 54 (Pt 1) (2021) 343–355.
[48] L. Zhang, P. Somasundaran, C. Maltesh, Electrolyte Effects on the Surface Tension and Micellization of n-Dodecyl β-d-Maltoside Solutions, Langmuir 12 (10) (1996) 2371–2373.
[49] A.M. de Vos, M. Ultsch, A.A. Kossiakoff, Human growth hormone and extracellular domain of its receptor: crystal structure of the complex, Science 255 (5042) (1992) 306–312.
[50] J.J. Adams, B.F. Anderson, G.E. Norris, L.K. Creamer, G.B. Jameson, Structure of bovine β-lactoglobulin (variant A) at very low ionic strength, J. Struct. Biol. 154 (3) (2006) 246–254.
[51] A.A. Spector, K. John, J.E. Fletcher, Binding of long-chain fatty acids to bovine serum albumin, J. Lipid Res. 10 (1) (1969) 56–67.
[52] A. Bujacz, Structures of bovine, equine and leporine serum albumin, Acta crystallographica, Section d, Biol. Crystallogr. 68 (Pt 10) (2012) 1278–1289.
[53] A. Micsonai, F. Wien, L. Kernya, Y.H. Lee, Y. Goto, M. Refregiers, J. Kardos, Accurate secondary structure prediction and fold recognition for circular dichroism spectroscopy, PNAS 112 (24) (2015) E3095–E3103.
[54] M.R. Eftink, Intrinsic Fluorescence of Proteins, in: J.R. Lakowicz (Ed.), Topics in Fluorescence Spectroscopy: Volume 6: Protein Fluorescence, Springer, US, Boston, MA, 2000, pp. 1–15.
[55] J.A. Reynolds, C. Tanford, Binding of Dodecyl Sulfate to Proteins at High Binding Ratios. Possible Implications for the State of Proteins in Biological Membranes*, Proceedings of the National Academy of Sciences 66(3) (1970) 1002-1007.
[56] S.P. Skinner, R.H. Fogh, W. Boucher, T.J. Ragan, L.G. Mureddu, G.W. Vuister, CcpNmr AnalysisAssign: a flexible platform for integrated NMR analysis, J. Biomol. NMR 66 (2) (2016) 111–124.
[57] J.D. Hines, R.K. Thomas, P.R. Garrett, G.K. Rennie, J. Penfold, Investigation of Mixing in Binary Surfactant Solutions by Surface Tension and Neutron Reflection: Anionic/Nonionic and Zwitterionic/Nonionic Mixtures, J. Phys. Chem. B 101 (45) (1997) 9215–9223.
[58] L. Zhang, P. Somasundaran, Adsorption of mixtures of nonionic sugar-based surfactants with other surfactants at solid/liquid interfaces: I. Adsorption of n-dodecyl-β-d-maltoside with anionic sodium dodecyl sulfate on alumina, J. Colloid Interface Sci. 302 (1) (2006) 20–24.
[59] E. Fegyver, R. Meszaros, The impact of nonionic surfactant additives on the nonequilibrium association between oppositely charged polyelectrolytes and ionic surfactants, Soft Matter 10 (12) (2014) 1953–1962.
[60] A. Sanchez-Fernandez, J. Hjalte, L. Porcar, H. Sjögren, S. Ulvenlund, M. Wahlgren, Studying the adsorption and desorption of surfactants onto proteins through the combination of in-situ dialysis and contrast variation SANS, Institut Laue-Langevin (ILL) (2021), https://doi.org/10.5291/ILL-DATA.9-13-948.
[61] A. Sanchez-Fernandez, J. Hjalte, R. Dalgliesh, C. Dicko, H. Sjögren, A.R. Rennie, M. Wahlgren, Direct observation of protein refolding in mixed surfactant systems using contrast variation SANS, ISIS Neutron and Muon Source (2021), https://doi.org/10.5286/ISIS.E.RB2010630.